

Root wood anatomy of 14 Brazilian Cerrado species

Anatomía de la madera de raíz de 14 especies del Cerrado Brasileño

Eduardo Luiz Longui ^{,} Juliana Arce de Goes Pacheco ^{a,} Sandra Monteiro Borges Florsheim ^{a,}
Gabriela Trindade Pires ^{a,} Julia Sonsin-Oliveira ^{b*}**

*Corresponding author: ^a Instituto Florestal, Divisão de Dasonomia, R. do Horto 931, CEP 02377-000, São Paulo, SP, Brazil, jsonsini@yahoo.com.br, edulongui@gmail.com

^b Universidade de Brasília - UNB, Campus Universitário Darcy Ribeiro, Instituto de Ciências Biológicas, Asa Norte, CEP 70910-900, Brasília, DF, Brazil.

SUMMARY

Studies on root wood anatomy are scarce, mainly due to the lack of commercial interest and the difficulty to collect. In Brazilian Cerrado, local craftsmen use root wood for marquetry, the manufacture of such small items as lampshades or ornaments, and table bases. However, taxonomy based on root wood can serve as a guide toward the conservation and management of tree stocks in urban environment. Therefore, we herein describe the root wood anatomy of 14 tree species that occur in the Brazilian Cerrado. To accomplish this, we studied samples from main sinker root, at a depth of about 20 cm, from 37 trees aged 5 to 10 years. Anatomical procedures followed the standard techniques for preparation and analyses of wood samples. We used stem or branch samples from other studies to carry out anatomical description and comparison. However, we encountered some problems, such as: difficulty to distinguish growth rings, sample processing and, in some cases, sample description, since quantity, distribution and type of axial parenchyma differed substantially from that of the main stem. Nonetheless, we did find a variation in the presence/absence of septate fibers among the samples, and noted differences in ray composition.

Key words: Cerrado species, tropical wood, wood identification, xylem anatomy.

RESUMEN

Los estudios sobre la anatomía de la madera de raíz son escasos, principalmente por la falta de interés comercial y la dificultad de recolección. En el Cerrado brasileño, los artesanos locales utilizan la madera de raíz para la marquetería, la fabricación de objetos pequeños como pantallas de lámparas o adornos, y la base de la mesa. Sin embargo, la taxonomía basada en la madera de raíz puede servir como una guía para la conservación y el manejo de las reservas de árboles en entornos urbanos. Por lo tanto, se describió la anatomía de la raíz de la madera de 14 especies de árboles que se encuentran en el Cerrado brasileño.

Se estudiaron muestras de la raíz principal, a una profundidad de aproximadamente 20 cm, de 37 árboles de 5 a 10 años. Los procedimientos anatómicos siguieron las técnicas estándar para la preparación y el análisis de muestras de madera. Se utilizaron muestras de tallo o rama de otros estudios para llevar a cabo la descripción anatómica y la comparación. Sin embargo, se encontraron algunos problemas, tales como: los anillos de crecimiento difíciles de distinguir; además, era problemático procesar la muestra y, en algunos casos, describirla dado que la cantidad, distribución y tipo de parénquima axial difería sustancialmente de la del tallo principal. No obstante, se encontró una variación en la presencia/ausencia de fibras septadas entre las muestras, y también diferencias en la composición de los radios.

Palabras clave: especies de Cerrado, madera tropical, identificación de madera, anatomía del xilema.

INTRODUCTION

Cerrado represents a vast tropical savanna ecoregion of Brazil, and woody species in this region are used by local populations for fuel and charcoal (Ratter *et al.* 1997). Local craftsmen are known to use root wood for marquetry, as well as for the manufacture of such small items as lampshades or ornaments. According to Krause *et al.* (2010), the scarcity of xylem research at root level can be explained by the lack of commercial interest. Besides, because

it is generally time-consuming and often costly (Maeght *et al.* 2013). However, apart from the use of root wood in crafts, the knowledge of root anatomy, irrespective of vegetation, can be very useful in instances where roots are the only evidence of such environmental crimes as deforestation. In urban settings, an analysis of roots following damage to underground pipes may help identify the offending trees from others.

Studies of root wood anatomy gain more prominence when comparisons are made between root wood and stem

wood regarding anatomy, wood properties, hydraulic conductivity and wood properties along axial variation within the tree. Such studies expand our knowledge of how such a variation occurs and the physiological and mechanical impact of such differences (Caldwell *et al.* 1998, Machado *et al.* 2007, Pratt *et al.* 2007, Longui *et al.* 2012, 2017, Fortunel *et al.* 2014, Marcati *et al.* 2014).

We acknowledge the difficulties involved in collecting samples of root wood in Cerrado species because of their sheer depth. Hence, the wood anatomy of roots from Cerrado species are largely unexplored, in addition many papers are focused in comparative wood anatomy (root versus stem or branches) and have only been reported on shrubs or small trees (Machado *et al.* 1997, Machado *et al.* 2007, Longui *et al.* 2012, 2017, Goulart and Marcati 2012, Marcati *et al.* 2014, Goulart *et al.* 2015).

Except for *Eriotheca gracilipes* roots studied by Longui *et al.* (2012) and *Anadenanthera peregrina*, *Copaifera langsdorffii*, *Handroanthus ochraceus*, *Ocotea corymbosa* and *Xylopia aromatica* roots studied by Longui *et al.* (2017), this is the first time we have a complete description for root anatomy of the selected species. Therefore, the present study contributes to fill a gap, especially by describing the root wood anatomy of 14 tree species that occur in the Brazilian Cerrado.

METHODS

Experimental area. The study was carried out in the Cerrado area of Assis State Forest (22°34'19" S, 50°23'32" W, ele-

vation 588 m), Assis, São Paulo. The soil in this region has low organic matter, although good water permeability. The climate is Cwa by the Köppen classification. Warm with dry winters, it is characterized by mean annual temperature of 20-25 °C (average minimum temperature of 18 °C) and average annual rainfall of 1,441.5 mm (CEPAGRI 2016). The dry season falls between April and September. Water deficit in April is -1.6 (sum of water deficit mm) and in August, it is -1.2 mm.

Collection of samples. We collected samples from 37 selected trees aged 5 to 10 years, comprising 14 tree species (table 1). We measured height and stem diameter at breast height (1.3 m from the ground) from each tree. To obtain root samples about 20 cm from the main sinker root, selected trees were uprooted. For standardization, anatomical studies were carried out on the wood portion adjacent to the cambium. Samples of 1.5 cm³ were cut from each disc.

Transverse and longitudinal radial and tangential sections, approximately 15 to 20 mm thick, were obtained. Sections were bleached in a solution of sodium hypochlorite and distilled water (50 %) and afterwards double-stained with aqueous 1 % safranin and aqueous 1 % astra blue (1:9) (Bukatsch 1972), followed by dehydration in an alcoholic series and, finally, passed through butyl acetate. To obtain cells dimensions, preparations of wood macerates were done according to Franklin's method (1945, modified by Kraus and Arduim 1997) and stained with aqueous 1 % safranin dye (Bukatsch 1972). Anatomical descriptions were based on the IAWA Committee (1989), for each fea-

Table 1. Studied species, number of samples, tree height and diameter at breast height (DBH).

Especies estudiadas, número de muestras, altura del árbol y diámetro a la altura de pecho (DAP).

Family	Species	N° samples	Height (m)	DBH (cm)
Annonaceae	<i>Xylopia aromatica</i> (Lam.) Mart.	4	4.2	4.8
Bignoniaceae	<i>Handroanthus ochraceus</i> (Cham.) Mattos	5	2.9	4.3
Erythroxylaceae	<i>Erythroxylum tortuosum</i> A. St.-Hil.	1	2.8	4.9
Fabaceae-Caesalpinoideae	<i>Copaifera langsdorffii</i> Desf.	5	4.0	4.5
Fabaceae-Mimosoideae	<i>Anadenanthera peregrina</i> var. <i>falcata</i> (Benth.) Altschul	3	3.4	5.6
	<i>Stryphnodendron adstringens</i> Benth.	2	3.0	5.1
Lauraceae	<i>Ocotea corymbosa</i> (Meisn.) Mez.	5	4.0	4.0
Malvaceae	<i>Eriotheca gracilipes</i> (K. Schum.) A. Robyns.	3	3.6	6.1
Melastomataceae	<i>Miconia albicans</i> (Sw.) Triana.	1	4.8	4.9
Myrtaceae	<i>Myrcia bella</i> Cambess.	2	4.1	8.1
	<i>Eugenia aurata</i> O. Berg.	2	1.9	3.5
	<i>Eugenia puniceifolia</i> (Kunth) DC.	2	3.1	2.9
Ochnaceae	<i>Ouratea spectabilis</i> (Mart.) Engl.	1	2.1	2.8
Vochysiaceae	<i>Vochysia tucanorum</i> Mart.	1	5.2	10.4

ture $n = 25$ was used initially, except for the pits, where $n = 10$ was adopted.

Qualitative and quantitative anatomical data were obtained with Image Pro Plus, v. 6.3, software attached to an Olympus CX 31 microscope.

RESULTS

Wood anatomical descriptions. Each species is described below and exemplified in figures 1-7; some details are in figure 8. All the quantitative values will be given as average and (maximum/minimum and standard deviation = SD).

Xylopia aromatica. Growth rings: marked by thick-walled and radially flattened latewood fibers (figure 1A, detail). Vessels: diffuse porosity, solitary and multiple (figure 1A); $437 \mu\text{m}$ ($613/155 \text{ SD} = 81$) in length, 15 per square milli-

meter (mm^{-2}) ($34/5 \text{ SD} = 7$), $79 \mu\text{m}$ ($137/31 \text{ SD} = 25$) in tangential diameter; simple perforation plate; intervessel pits alternate, circular; vessel-ray pits similar to intervessel pits in size and shape; few deposits. Fibers: with distinctly bordered pits (less than $3 \mu\text{m}$) (figure 8A); thin-to thick-walled; $880 \mu\text{m}$ ($1455/534 \text{ SD} = 166$) in length. Axial parenchyma: predominantly scalariform, and in irregular lines, sometimes reticulate (figure 1A); 2 to 5 cells per parenchyma strand. Rays: 1 to 6 cells wide (figure 1B); $462 \mu\text{m}$ ($1087/172 \text{ SD} = 192$) tall, $59 \mu\text{m}$ ($118/24 \text{ SD} = 55$) wide, $11/\text{mm}$ ($16/5 \text{ SD} = 2$), all ray cells procumbent; body ray cells procumbent with one row of upright and/or square marginal cells (figure 1C); secretory elements: oil cells associated with ray and axial parenchyma (figure 1B,C, arrowhead). Aggregate rays in 1B.

Handroanthus ochraceus. Growth rings: marked by marginal bands of axial parenchyma, sometimes more than 10 cells wide, and occasionally by lines (figure 1D, detail), high quantity of vessels adjacent to the growth layer can occur. Vessels: diffuse porosity; solitary and multiple vessels (figure 1D); $227 \mu\text{m}$ ($350/130 \text{ SD} = 47$) in length, 25 per square millimeter (mm^{-2}) ($113/6 \text{ SD} = 25$), $79 \mu\text{m}$ ($130/38 \text{ SD} = 18$) in tangential diameter; simple perforation plate; intervessel pit alternate, circular; vessel-ray pits similar to intervessel pits in size and shape. Fibers: very thick-walled; $903 \mu\text{m}$ ($1354/294 \text{ SD} = 270$) in length; with simple to minutely bordered pits; gelatinous fibers may occur. Axial parenchyma: unilateral, short to long confluent forming irregular bands, lozenge-aliform and marginal bands (figure 1D); mostly with 2 to 4, or rarely 6, cells per parenchyma strand. Rays: 1 to 2 cells wide (figure 1E); $145 \mu\text{m}$ ($293/66 \text{ SD} = 33$) tall, $18 \mu\text{m}$ ($36/7 \text{ SD} = 5$) wide, $6/\text{mm}$ ($14/3 \text{ SD} = 2$); all ray cells procumbent (figure 1F); perforated ray cells. Storied structure: axial parenchyma regularly storied; rays regular to irregularly storied (figure 1E).

Erythroxylum tortuosum. Growth rings: marked by fiber zones (figure 2A, arrow). Vessels: diffuse-porous; solitary and multiples (figure 2A); $331 \mu\text{m}$ ($477/205 \text{ SD} = 69$) in length, 33 per square millimeter (mm^{-2}) ($57/18 \text{ SD} = 10$), $73 \mu\text{m}$ ($88/60 \text{ SD} = 8$) in tangential diameter; simple perforation plates; intervessel pits alternate, circular; vessel-ray pits similar to intervessel pits in size and shape throughout and pits with many reduced borders to apparently simple, horizontal to vertical; tyloses; deposits. Fibers: fibers with distinctly bordered pits (figure 8B); very thick-walled; $763 \mu\text{m}$ ($952/538 \text{ SD} = 104$) in length; gelatinous fibers. Axial parenchyma: diffuse-in-aggregates, diffuse, unilateral and scanty paratracheal (figure 2A); 2 to 8 cells per parenchyma strand. Rays: 1 to 3 ray cells in width; $271 \mu\text{m}$ ($477/205 \text{ SD} = 45$) tall, $35 \mu\text{m}$ ($46/25 \text{ SD} = 5$) wide, $10/\text{mm}$ ($14/5 \text{ SD} = 2$); uniseriate portion as wide as multiseriate portions (figure 2B); body ray cells procumbent with 2-4 rows of upright and/or square marginal cells and square and upright cells mixed throughout the ray (figure 2C). In-

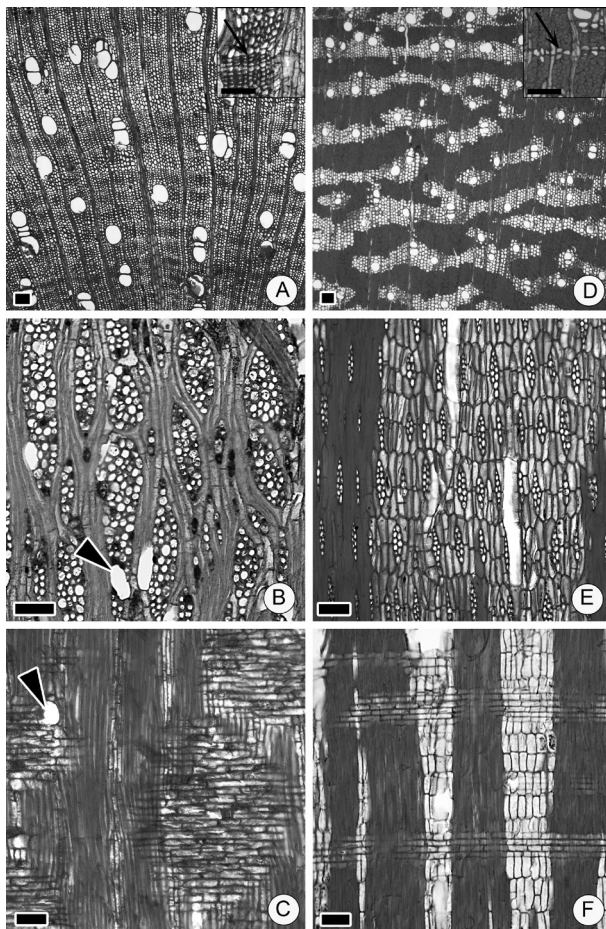


Figure 1. Root wood anatomical features of *Xylopia aromatica* (A-C); arrow points growth ring in A, detail; arrow points oil cell in C; and *Handroanthus ochraceus* (D-F); arrow points growth ring in D, detail. Scale bars = $100 \mu\text{m}$; details = $50 \mu\text{m}$.

Características anatómicas de la madera de raíz de *Xylopia aromatica* (a-c) y *Handroanthus ochraceus* (D-F). Barras = $100 \mu\text{m}$; detalles = $50 \mu\text{m}$.

organic inclusions: prismatic crystals in chambered axial parenchyma cells and in ray cells.

Copaifera langsdorffii. Growth rings: marked by marginal bands of axial parenchyma (figure 2D, arrows). Vessels: diffuse-porous; solitary and multiple (figure 2D); 416 μm (880/121 SD = 118) in length, 17 per square millimeter (mm^{-2}) (25/3 SD = 4), 83 μm (215/35 SD = 30) in tangential diameter; simple perforation plate; intervessel pits alternate, circular, vestured; vessel-ray pits similar to intervessel pits in size and shape; deposits. Fibers: with simple to minutely bordered pits; thin- to very thick-walled; 891 μm (1896/150 SD = 267) in length. Axial parenchyma: in bands, lozenge and short confluent; 2 to 4 cells per parenchyma strand (figure 2D). Rays: 1 to 5 cells wide (figure 2E); 299 μm (1030/84 SD = 145) tall, 50 μm (89/10 SD = 17) wide, 7/mm (10/4 SD = 1); all ray

cells procumbent; body ray cells procumbent with one to two rows of upright and/or square marginal cells (figure 2F). Secretory structures: axial canal in long tangential lines (figure 2D - arrow head; figure 8C - arrow). Inorganic inclusions: prismatic crystals in chambered axial parenchyma cells.

Anadenanthera peregrina var. *falcata*. Growth rings: marked by axial parenchyma flattened cells and by flattened latewood fibers (figure 3A, detail). Vessels: diffuse-porous; solitary and multiples of three (figure 3A) and some up to six; 251 μm (386/117 SD = 55) in length, 14 per square millimeter (mm^{-2}) (39/7 SD = 5), 90 μm (211/55 SD = 35) in tangential diameter; simple perforation plates; intervessel pits alternate, circular, vestured; vessel-ray pits similar to intervessel pits in size and shape, and with many reduced

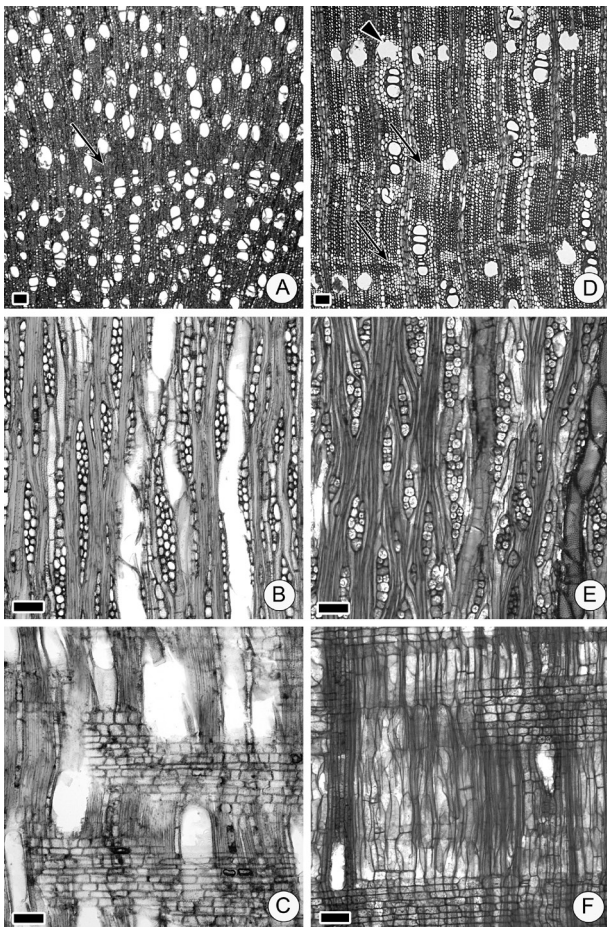


Figure 2. Root wood anatomical features of *Erythroxylum tortuosum* (A-C) and *Copaifera langsdorffii* (D-F); arrows point growth ring in A and D, detail. Scale bars = 100 μm ; details = 50 μm .

Características anatómicas de la madera de raíz de *Erythroxylum tortuosum* (A-C) y *Copaifera langsdorffii* (D-F). Barras = 100 μm ; detalles = 50 μm .

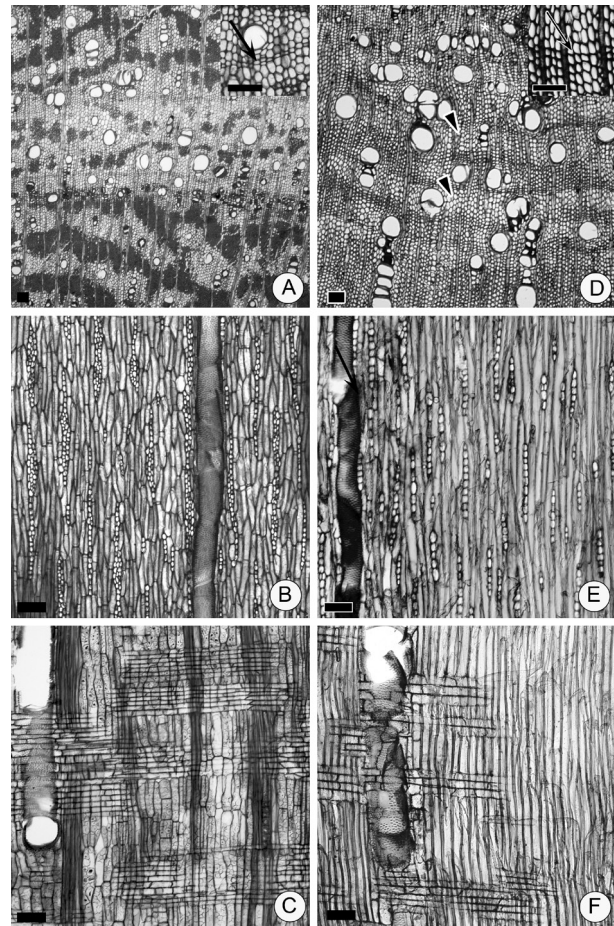


Figure 3. Root wood anatomical features of *Anadenanthera peregrina* var. *falcata* (A-C) and *Stryphnodendron adstringens* (D-F); parenchyma-like fiber bands alternating with ordinary fibers (arrow head); arrows point growth ring in A and D, detail. Scale bars = 100 μm ; details = 50 μm .

Características anatómicas de la madera de raíz de *Anadenanthera peregrina* var. *falcata* (A-C) y *Stryphnodendron adstringens* (D-F). Barras = 100 μm ; detalles = 50 μm .

borders to apparently simple, rounded; deposits. Fibers: simple to minutely bordered pits; very thick-walled; 1311 μm (2197/681 SD = 340) in length; gelatinous fibers in small groups, sometimes forming bands intercalating with the axial parenchyma. Axial parenchyma: predominantly in bands more than three cells wide, long confluent, few short confluent and lozenge (figure 3A); 2 to 4 cells per parenchyma strand; great quantity of starch. Rays: 1 to 3 ray cells in width (figure 3B); 195 μm (442/92 SD = 68) tall, 28 μm (47/9 SD = 8) wide, 6/mm (12/4 SD = 2); all ray cells procumbent (figure 3C). Inorganic inclusions: prismatic crystals in chambered axial parenchyma cells and in fibers.

Stryphnodendron adstringens. Growth rings: poorly marked by flattened latewood fibers (figure 3D, detail). Vessels: solitary and multiples (figure 3D); 351 μm (521/190 SD = 81) in length, 11 per square millimeter (mm^{-2}) (34/1 SD = 7), 127 μm (184/78 SD = 24) in tangential diameter; simple perforation plate; intervessel pits alternate, circular and vestured; vessel-ray pits similar to intervessel pits in size and shape; deposits. Fibers: thin-walled; 639 μm (884/441 SD = 112) in length; with simple to minutely bordered pits; septate; parenchyma-like fiber bands alternating with ordinary fibers (figure 3D, arrow head). Axial parenchyma: vasicentric and few lozenge (figure 3D); 2 to 4 cells per parenchyma strand. Rays: uniseriate and few locally biseriate (figure 3E); 364 μm (748/169 SD = 155) tall, 36 μm (67/13 SD = 17) wide, 6/mm (10/2 SD = 2); all ray cells procumbent, and few body ray cells procumbent with one row of upright and/or square marginal cells (figure 3F). Inorganic inclusions: prismatic crystals in chambered fibers. Pith flecks: present (figure 8D).

Ocotea corymbosa. Growth rings: marked by radially flattened latewood fibers (figure 4A, detail). Vessels: diffuse-porous; solitary and multiples (figure 4A); 613 μm (1737/233 SD = 319) in length, 13 per square millimeter (mm^{-2}) (24/4 SD = 4), 117 μm (216/63 SD = 29) in tangential diameter; simple perforation plates; intervessel pits alternate, circular; vessel-ray pits with many reduced borders to apparently simple, pits rounded, horizontal to vertical, and two types in the same ray cell; tyloses. Fibers: thin-walled; 1000 μm (1462/624 SD = 222) in length; simple to minutely bordered pits; septate; parenchyma-like fiber bands alternating with ordinary fibers (figure 4A, arrow head). Axial parenchyma: scanty paratracheal (figure 4A); 3 to 7 cells per parenchyma strand; few vasicentric. Rays: 1 to 3, and few up to 6 cells wide (figure 4B); 491 μm (972/176 SD = 180) tall, 54 μm (84/27 SD = 12) wide, 6/mm (8/3 SD = 1); body ray cells procumbent with one row upright and/or square, and few 2-4 rows; rays with procumbent, square (figure 4C) and upright cells mixed throughout the ray. Secretory elements: oil cells associated with ray parenchyma and fibers (figure 4 B and C, arrows).

Eriotheca gracilipes. Growth rings: poorly marked by flattened latewood fibers (figure 4D). Vessels: diffuse porosity; solitary and multiple (figure 4D); 362 μm (549/204 SD = 66) in length, 2 per square millimeter (mm^{-2}) (6/0 SD = 1), 174 μm (266/93 SD = 39) in tangential diameter; simple perforation plate; intervessel pits alternate, circular; vessel-ray pits with many reduced borders to apparently simple, rounded and similar to intervessel pits in size and shape; tyloses. Fibers: few fibers (very thick-walled) embedded in parenchyma cells; 1784 μm (3996/975 SD = 464) in length; with distinctly bordered pits (less than 3 μm); septate. Axial parenchyma: apparently in bands given the few fibers (figure 4D); 2 to 5 cells per parenchyma strand. Rays: few 1 to 3 and mostly wider than 10-seriate by the relative absence of fibers (figure 4E); sheath cells (figure 4E, arrow); with procumbent, square and upright

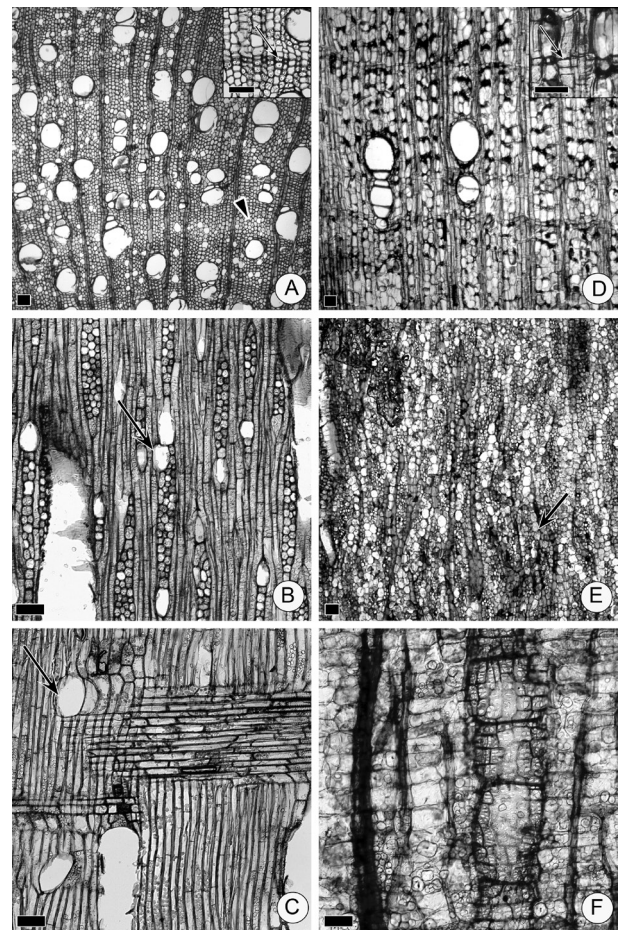


Figure 4. Root wood anatomical features of *Ocotea corymbosa* (A-C); parenchyma-like fiber bands alternating with ordinary fibers (arrow head) (A); and *Eriotheca gracilipes* (D-F); arrows point growth ring in A and D, detail. Scale bars = 100 μm ; details = 50 μm .

Características anatómicas de la madera de raíz de *Ocotea corymbosa* (A-C) y *Eriotheca gracilipes* (D-F). Barras = 100 μm ; detalles = 50 μm .

cells mixed throughout the ray (figure 4F); perforated ray cells. Ray measurements in the root were not performed due to difficulty in visualizing the ray cells that overlapped with the parenchyma cells that occur on a large scale, associated with the tiny proportion of fibers and vessels. Inorganic inclusions.

Miconia albicans. Growth rings: marked by thick-walled and radially flattened latewood fibers (figure 5A, detail). Vessels: diffuse porosity; solitary and multiple (figure 5A); 398 μm (1233/129 SD = 203) in length, 41 per square millimeter (mm^{-2}) (66/20 SD = 8), 37 μm (129/13 SD = 36) in tangential diameter; simple perforation plate; intervessel pits alternate, circular and vested; vessel-ray pits similar to intervessel pits in size and shape; deposits. Fibers: very thin- to thick-walled; septate; 1300 μm (2239/769 SD = 297)

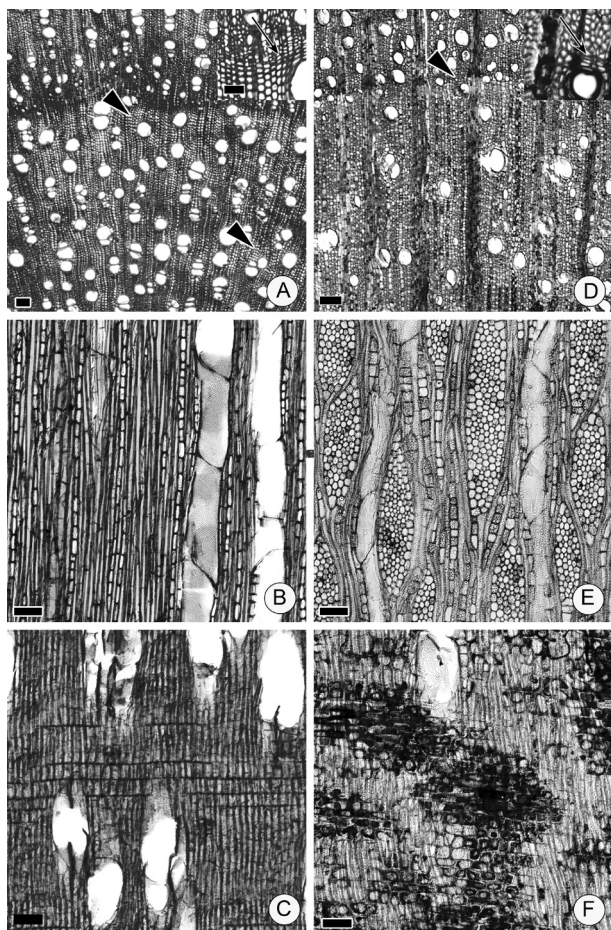


Figure 5. Root wood anatomical features of *Miconia albicans* (A-C); parenchyma-like fiber bands alternating with ordinary fibers (arrow head) (A); and *Myrcia bella* (D-F); arrows point growth ring in A and D, detail wood. Scale bars = 100 μm ; details = 50 μm .

Características anatómicas de la madera de raíz de *Miconia albicans* (A-C) and y *Myrcia bella* (D-F). Barras = 100 μm ; detalles = 50 μm .

length; parenchyma-like fiber bands alternating with ordinary fibers (figure 5A); gelatinous fibers. Axial parenchyma: scanty (figure 5A); 3 to 5 cells per parenchyma strand; 488 μm (658/321 SD = 83) tall, 24 μm (32/18 SD = 3) wide, 7/mm (11/5 SD = 1); Rays: exclusively uniseriate (figure 5B); all ray cells upright and/or square (figure 5C).

Myrcia bella. Growth rings: marked by thick-walled and radially flattened latewood fibers (figure 5D, arrow head). Vessels: diffuse porosity; exclusively solitary (figure 5D); 632 μm (797/451 SD = 86) in length, 6 per square millimeter (mm^{-2}) (11/2 SD = 2), 82 μm (123/58 SD = 17) in tangential diameter; simple perforation plate; intervessel pits alternate, circular and vested; vessel-ray pits similar to intervessel pits in size and shape. Fibers: with distinctly bordered pits (figure 8E); thin- to thick-walled; 1085 μm (1355/833 SD = 150) in length; few with septa. Axial parenchyma: diffuse-in-aggregates and scanty (figure 5D); 2 to 6 cells per parenchyma strand. Rays: uniseriate and 1 to 7 cells wide, with two distinct sizes (figure 5E); 455 μm (577/341 SD = 69) tall, 60 μm (79/46 SD = 9) wide, 8/mm (10/5 SD = 1), measurements refer to multiseriate rays; body ray cells procumbent with mostly 2 to more than 4 rows of upright and/or square marginal cells; all ray cells upright and/or square (figure 5F); perforated ray cells. Aggregated rays.

Eugenia aurata. Growth rings: marked by fiber zones and higher frequency of vessels adjacent to the growth rings (figure 6A, detail). Vessels: diffuse porosity; solitary and few multiple (figure 6A); 424 μm (572/287 SD = 79) in length, 127 per square millimeter (mm^{-2}) (165/67 SD = 26), 36 μm (49/28 SD = 5) in tangential diameter; simple perforation plate; intervessel pits alternate, circular, vested; vessel-ray pits similar to intervessel pits in size and shape; few deposits. Fibers: with distinctly bordered pits (figure 8F); very thick-walled; 951 μm (1163/678 SD = 124) in length; gelatinous fibers. Axial parenchyma: diffuse-in-aggregates forming lines and diffuse (figure 6A); predominantly 4 to 8 cells, and some more than 8 cells per parenchyma strand. Rays: 1 to 3 ray cells in width (figure 6B); 298 μm (425/209 SD = 45) tall, 38 μm (49/25 SD = 5) wide, 12/mm (16/8 SD = 2); predominantly with body ray cells procumbent with over 4 rows of upright and/or square marginal cells; few having all one row of upright and/or square marginal cells; and square and upright cells mixed throughout the ray (figure 6C). Inorganic inclusions: prismatic crystals in enlarged cells.

Eugenia puniceifolia. Growth rings: marked by fiber zones (figure 6D, detail). Vessels: diffuse porosity; solitary and few multiple (figure 6D); 519 μm (767/233 SD = 126) in length, 86 per square millimeter (mm^{-2}) (146/46 SD = 22), 43 μm (58/24 SD = 7) in tangential diameter; intervessel pits alternate, circular and vested; vessel-ray pits similar to intervessel pits in size and shape; deposits. Fibers: with

distinctly bordered pits (figure 8G); very thick-walled; 788 μm (1182/591 SD = 122) in length. Axial parenchyma: diffuse-in-aggregates forming lines (figure 6D); 4 to 8 cells per parenchyma strand. Rays: 1 to 3 cells wide (figure 6E); 434 μm (652/276 SD = 85) tall, 46 μm (68/24 SD = 8) wide, 7/mm (11/4 SD = 1); with uniseriate portion as wide as multiseriate portions (figure 6E); body ray cells procumbent with one to over 4 rows of upright and/or square marginal cells (figure 6F), and rays with procumbent, square and upright cells mixed throughout the ray; perforated ray cells.

Ouratea spectabilis. Growth rings: marked by fiber zones (figure 7A, detail). Vessels: diffuse porosity; exclusively solitary (figure 7A); 547 μm (773/334 SD = 122) in length, 13 per square millimeter (mm^{-2}) (19/9 SD = 2), 55 μm (69/41 SD = 7) in tangential diameter; simple perforation plate; intervessel pits alternate, circular; vessel-ray pits si-

milar to intervessel pits in size and shape; few deposits. Fibers: with distinctly bordered pits (figure 8I); very thick-walled; few septate (figure 8H); 1331 μm (1832/888 SD = 249) in length. Axial parenchyma: diffuse and diffuse-in-aggregates, scanty paratracheal (figure 7A); 2 to 6 cells per parenchyma strand. Rays: 1-seriate and larger rays to 6 cells wide (figure 7B); 1058 μm (1796/605 SD = 257) tall, 101 μm (153/60 SD = 19) wide, 5/mm (7/3 SD = 1); of two distinct sizes, measurements refer to multiseriate rays; with procumbent, square and upright cells mixed throughout the ray (figure 7C); all ray cells upright and/or square. Inorganic inclusions: prismatic crystals in square ray cells.

Vochysia tucanorum. Growth rings: indistinct. Vessels: diffuse porosity; solitary and multiple (figure 7D); 465 μm (707/274 SD = 112) in length, 11 per square millimeter (mm^{-2}) (25/6 SD = 4), 155 μm (232/96 SD = 31) in tangential diameter; simple perforation plate; intervessel pits

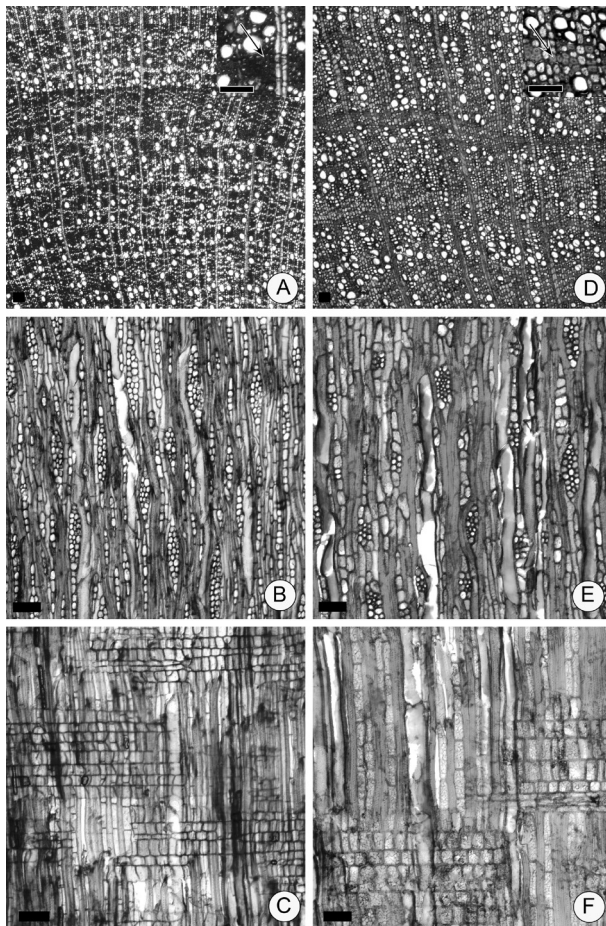


Figure 6. Root wood anatomical features of *Eugenia aurata* (A-C) and *Eugenia puniceifolia* (D-F); arrows point growth ring in A and D, detail. Scale bars = 100 μm ; details = 50 μm .

Características anatómicas de la madera de raíz de *Eugenia aurata* (A-C) y *Eugenia puniceifolia* (D-F). Barras = 100 μm ; detalles = 50 μm .

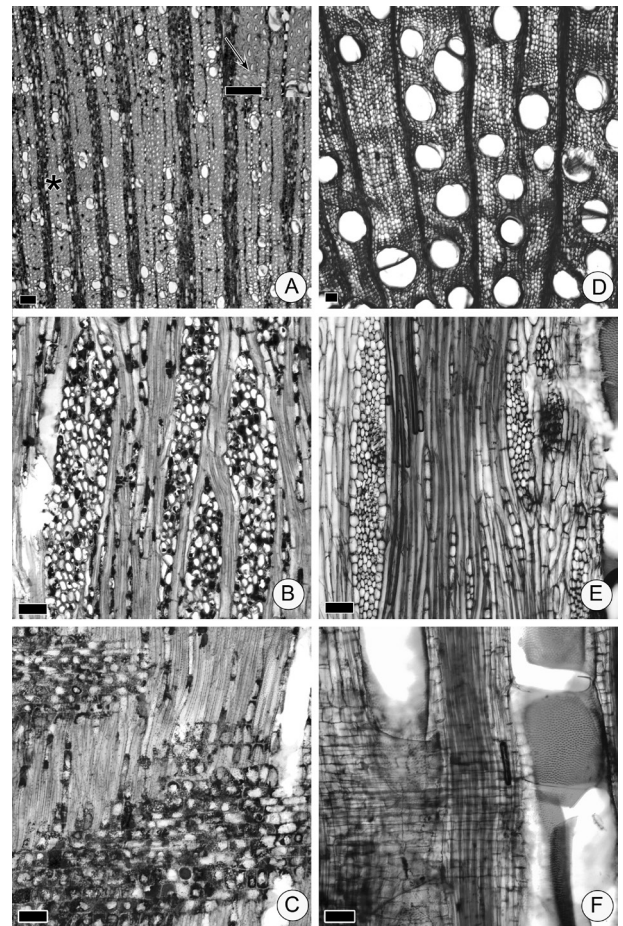


Figure 7. Root wood anatomical features of *Ouratea spectabilis* (A-C) arrow points growth ring in (A), detail and *Vochysia tucanorum* (D-F). Scale bars = 100 μm ; details = 50 μm .

Características anatómicas de la madera de raíz de *Ouratea spectabilis* (A-C) y *Vochysia tucanorum* (D-F). Barras = 100 μm ; detalles = 50 μm .

alternate, circular, vested; vessel–ray pits similar to inter-vessel pits in size and shape; deposits. Fibers: with simple to minutely bordered pits; thin- to very thick-walled; septate; 1266 μm (1578/758 SD = 228) in length. Axial parenchyma in bands more than 3 cells wide (figure 7D); 2 to 6 cells per parenchyma strand. Rays: 3 to 7 cells wide, few uniseriate (figure 7E); 937 μm (1293/657 SD = 148) tall, 85 μm (125/46 SD = 18) wide, 4/mm (6/2 SD = 1) of two distinct sizes, measurements refer to multiseriate rays; sheath cells (figure 7E); body ray cells procumbent with one to 4 rows of upright and/or square marginal cells (figure 7F); all rays upright and/or square, and rays with procumbent, square and upright cells mixed throughout the ray.

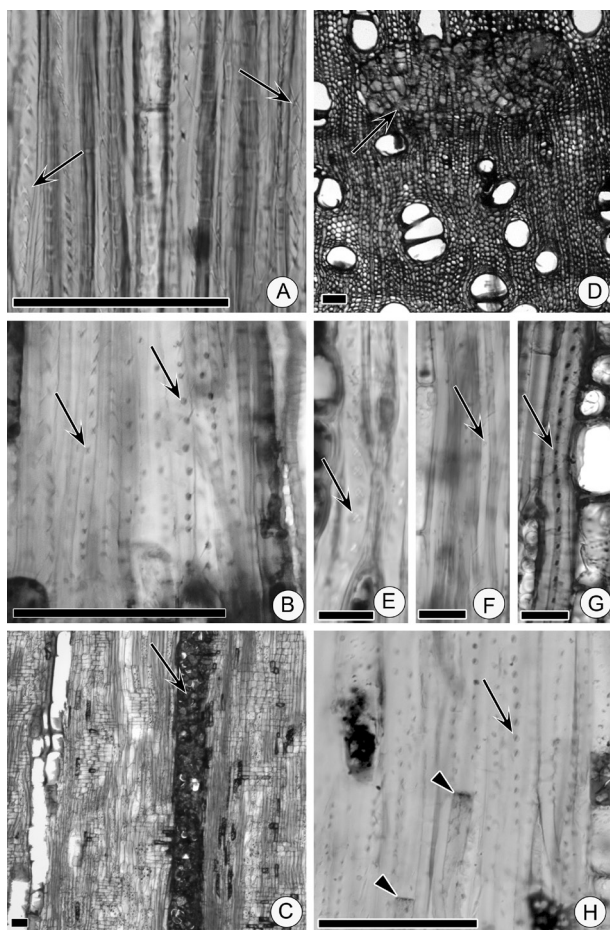


Figure 8. Root wood anatomical features. *Xylopi aromaticata* fiber pits (A) in TLS, arrows; detail in macerate; *Erythroxyllum tortuosum* fiber pits in RLS (B), arrows; *Copaifera langsdorffii* axial canal in RLS (C), arrow; *Stryphnodendron adstringens* pith flecks (arrow) TS (D); fiber pits (arrow) in: *Myrcia bella* in TLS (E), *Eugenia aurata* in RLS (F), *Eugenia puniceifolia* in TLS (G), *Ouratea spectabilis* and septate fiber (arrow head) (H) in RLS. Scale bars A-D;H = 100 μm ; E-G and details = 25 μm .

Características anatómicas de la madera de raíz de *Ouratea spectabilis* (A-C) y *Vochysia tucanorum* (D-F). Barras A-D;H = 100 μm ; E-G y detalles = 25 μm .

DISCUSSION

Qualitative wood anatomical descriptions of roots were compared with literature for main stem or branch wood for the same species and, when possible, with Cerrado species from São Paulo, using the work of Sonsin *et al.* (2014) and InsideWood, a Web resource (2016), containing descriptions of wood anatomy from different biomes of Brazil, or other countries, and many authors.

According to Sonsin *et al.* (2014) studying stem wood, growth rings are not as easy to interpret as they are in temperate woods. The authors also stand out that the growth ring markers are more easily observed at low magnification with the naked eye or using a hand lens than under the microscope. While analyzing roots we noticed growth rings, in general, are harder to distinguish than the main stem or branch because of the quantity and distribution of axial parenchyma, which consequently complicated description. In some cases, there were islands of fibers among the axial parenchyma cells as in *Anadenanthera peregrina* var. *falcata* and *Vochysia tucanorum*, very different from the branch or main stem (see Sonsin *et al.* 2014 and InsideWood).

The higher quantity of axial parenchyma observed in roots and the presence of septate fibers in some roots (*Erythroxyllum tortuosum*, *Sthyphnodendron adstringens*, *Eriotheca gracilipes*, *Ouratea spectabilis* and *Vochysia tucanorum* species), although not in stem or branches (see Sonsin *et al.* 2014 and InsideWood), may indicate an evolutionary adjustment to provide for more storage tissue (Dickson 2000).

The root wood anatomical data of *Xylopi aromatica* were similar to those cited by Detienne and Jacquet (1983) at stem wood; however, the axial parenchyma was not as well defined as that in stem wood, essentially because of the high quantity of axial parenchyma in root wood where lines are not clearly scalariform. Furthermore; ray composition is highly varied.

For *Handroanthus ochraceus*, we observed growth rings well marked by marginal bands of axial parenchyma, different from the observation of Teixeira *et al.* (2003), who reported indistinct growth rings at stem level. Again, in this species, we observed variation in the quantity of axial parenchyma, mostly very large bands more than 10 cells wide. Even, the storied structure was not always regular.

Generally, the anatomical root features of *Erythroxyllum tortuosum* were similar to those of stem wood (see Sonsin *et al.* 2014), however, the fibers are very thick-walled in this study, while in Sonsin *et al.* (2014), the fibers were thin- to thick-walled. The author noted variation in ray composition, whereas in the present study, we noted body ray cells procumbent with 2-4 rows of upright and/or square marginal cells. In addition, we reported only square and upright cells mixed throughout the ray, whereas Sonsin *et al.* (2014) reported procumbent, square and upright

Table 2. Comparison of qualitative anatomical features of roots in the present study (#) and among qualitative anatomical features of stem by Sonsin *et al.* (2014) (*) and Inside Wood information (†).

Comparación de las características anatómicas cualitativas de las raíces en el presente estudio (#) y entre las características anatómicas cualitativas del tallo por Sonsin *et al.* (2014) (*) e información de Inside Wood (†).

Species	Tracheids			Fiber with distinct borders			Septate			Parenchyma-like fibre			Rays - distinct sizes			Crystals			Perforated ray cells		
	#	*	†	#	*	†	#	*	†	#	*	†	#	*	†	#	*	†	#	*	†
<i>Xylopia aromatica</i>	0	-	0	3	-	1	0	-	0	0	-	0	0	-	0	0	-	0	1	-	1
<i>Handroanthus ochraceus</i>	0	-	-	0	-	0	0	-	0	0	-	0	0	-	0	0	-	0	1	1	0
<i>Erythroxylum tortuosum</i>	0	1	-	1	1	-	-	0	-	0	-	0	0	-	0	0	-	0	0	-	1
<i>Copaifera langsdorffii</i>	0	0	0	0	0	0	0	0	0	0	0	0	0	0	0	0	0	0	1	1	0
<i>Anadenanthera peregrina</i> var. <i>falcata</i>	0	0	-	0	0	-	0	0	0	0	0	0	0	0	0	0	0	0	1	1	0
<i>Stryphnodendron adstringens</i>	0	0	0	0	0	0	1	0	0	1	0	0	0	0	0	0	0	0	1	1	0
<i>Ocotea corymbosa</i>	0	0	-	0	0	-	1	1	-	1	1	-	0	0	0	0	-	0	0	0	0
<i>Eriotheca gracilipes</i>	0	0	-	3	0	-	1	0	-	0	0	-	0	1	-	0	0	0	1	1	1
<i>Miconia albicans</i>	0	0	-	0	0	-	1	1	-	1	1	-	0	0	0	0	-	0	0	0	0
<i>Myrcia bella</i>	0	1	-	0	0	0	4	0	0	0	0	0	1	0	0	0	0	0	1	1	1
<i>Eugenia aurata</i>	0	-	1	1	1	1	1	0	0	0	0	0	0	0	0	0	0	0	1	1	0
<i>Eugenia puniceifolia</i>	0	-	1	1	1	1	0	0	0	0	0	0	0	0	0	0	0	0	1	1	1
<i>Ouratea spectabilis</i>	0	0	0	1	1	1	1	0	0	0	0	0	0	0	0	1	1	1	1	1	0
<i>Lochysia tucanorum</i>	0	0	0	0	0	0	1	0	0	0	0	0	0	0	1	1	1	1	1	1	0

1 = present; - = no species information; 0 = absent; 3 = fiber with bordered pit, but less than 3µm; 4 = few.

(#) studied species in the present study.

(*) Sonsin *et al.* (2014) (*Stryphnodendron polyphyllum*, *Eugenia bimarg* and *E. rigida*).

(†) Inside Wood (*Handroanthus impetiginosus* and *H. serratifolius*, *Anadenanthera peregrina*, *Eugenia lucida* and *E. tinifolia* (spp.), *Ouratea castaneaefolia*, *Lochysia lanceolata* and *L. ferruginea*).

cells mixed throughout the ray. Finally, we observed prismatic crystals in chambered axial parenchyma cells.

The general anatomical features of *Copaifera langsdorffii* were similar to those noted in literature for main stem and branch (Richter and Dallwitz 2000, Sonsin *et al.* 2014), nonetheless we observed variation in ray composition with all ray cells procumbent and body ray cells procumbent with one to two rows of upright and/or square marginal cells. In contrast, only one or two rows of upright and/or marginal cells have, thus far, been noted in the literature.

For *Anadenanthera peregrina* var. *falcata*, we observed a great variation in the quantity of paratracheal parenchyma, either in bands or long confluent, with fibers appearing to be embedded within axial parenchyma cells when compared to stem studied by Sonsin *et al.* (2014).

For *Stryphnodendron adstringens*, the main difference observed was the presence of parenchyma-like fiber bands alternating with ordinary fibers when compared to root wood studied by Goulart *et al.* (2015) and wood stem studied by Montefusco (2005). In the present study, fibers were septate. According to Goulart *et al.* (2015), prismatic crystals were observed in fibers and in chambered axial parenchyma cells.

For *Ocotea corymbosa*, we observed variation in ray composition and thickness of fibers when compared to Paula *et al.* (2000), studying stem wood of gallery forest species. Our observations are more in line with those of Sonsin *et al.* (2014) in both axial and radial parenchyma.

For *Eriotheca gracilipes*, we observed a few very thick-walled fibers which seem to be embedded in parenchyma cells that occur in large bands, not diffuse-in-aggregates, forming lines, as in the stem wood observed by Sonsin *et al.* (2014). Also, growth rings were very difficult to see in roots in this study, while in Longui *et al.* (2012) and Marcati *et al.* (2006), thick-walled and radially flattened latewood fibers were noted at the main stem and branch.

The anatomical description of *Miconia albicans* was similar to that of Sonsin *et al.* (2014) at stem level.

Compared to Sonsin *et al.* (2014), the description of *Myrcia bella* differed only in the presence of a few septate fibers present in roots, while tracheids were only observed in branches.

We did not find a basis for comparison of either *Eugenia aurata* or *E. puniceifolia*. However, apart from variation in the presence or absence and size of prismatic crystals, the anatomical features are like the genera described by Soffiatti and Angyalossy-Alfonso (1999) and Sonsin *et al.* (2014).

For *Ouratea spectabilis*, the fibers were thicker in roots compared to Sonsin *et al.* (2014). We observed variation in ray composition, with procumbent, square and upright cells mixed throughout the ray in both papers, we also found all ray cells to be upright and/or square.

We did not observe the presence of growth rings in *Vochysia tucanorum*, nevertheless we did note septate fibers,

whereas Sonsin *et al.* (2014) did not. The high quantity of axial parenchyma, which forms sinuous bands, was variable, being higher in roots, while in branches, paratracheal parenchyma varied, with less quantity, though. We saw variation in ray composition when compared to Sonsin *et al.* (2014), with more rows and rays with mixed up cells. Paula *et al.* (2000) observed only homogeneous rays and included phloem, which was not observed in the present work or that of Sonsin *et al.* (2014).

CONCLUSIONS

In general, the quantity and distribution of axial parenchyma of root wood are very different from that of the main stem, being higher in roots, in which we concluded that the roots main function is not focused on support, but on storage. This same quantity of axial parenchyma in root wood made it difficult to describe; growth rings are hard to distinguish.

ACKNOWLEDGMENTS

The authors thank Yara R. W. Vianello for laboratory assistance and Antônio C. G. de Melo for fieldwork. We also thank the Conselho Nacional de Desenvolvimento Científico e Tecnológico - CNPq (National Council for Scientific and Technological Development - 145829/2012-0 and 121304/2013-2) for grants to Gabriela T. Pires and the Fundação do Desenvolvimento Administrativo (FUN-DAP) for the grant to Juliana Arce de Goes Pacheco.

REFERENCES

- Bukatsch F. 1972. Bemerkungen zur Doppelfärbung Astrablau-Safranin. *Mikrokosmos* 61(8): 255.
- Caldwell MM, TE Dawson, JH Richards. 1998. Hydraulic lift: consequences of water efflux from the roots of plants. *Oecologia* 113(2):151-161.
- CEPAGRI (Centro de Pesquisas Meteorológicas e Climáticas Aplicadas a Agricultura, BR). Clima dos Municípios Paulistas. Accessed 18 Sep. 2016. Available in <http://www.cpa.unicamp.br/outras-informacoes/clima-dos-municipios-paulistas.html>
- Detienne P, P Jacquet. 1983. Atlas d'identification des bois de l'amazonie et des regions voisines. Nogent-sur-Marne, France. Centre Technique Forestier Tropical. 640 p.
- Fortunel C, J Ruelle, J Beauchene, PVA Fine, C Baraloto. 2014. Wood specific gravity and anatomy of branches and roots in 113 Amazonian rainforest tree species across environmental gradients. *New Phytologist* 202(1):79-94. [doi/10.1111/nph.12632](https://doi.org/10.1111/nph.12632)
- Franklin G. 1945. Preparations of thin sections of synthetic resins and wood - resin composites and a new macerating method for wood. *Nature* 155:51.
- Goulart SL, AO Ribeiro, FA Mori, NF Almeida, CO Assis. 2015. Anatomia do lenho de raiz, tronco e galho de barbatimão (*Stryphnodendron adstringens* (Mart) Coville). *Cerne* 21(2):329-338. doi.org/10.1590/01047760201521021627

- Goulart SL, CR Marcati. 2008. Anatomia comparada do lenho em raiz e caule de *Lippia salviifolia* Cham. (Verbenaceae). *Revista Brasileira de Botânica* 31(2):263-275.
- IAWA Committee. 1989. IAWA list of microscopic features for hardwood identification. *IAWA Bulletin* 10(2):219-332.
- Inside Wood - NC State University. accessed 24 Aug. 2016. Available in <http://insidewood.lib.ncsu.edu>
- Kraus JE, M Arduin. 1997. Manual básico de métodos em morfologia vegetal. Rio de Janeiro, Brazil. EDUR. 198 p.
- Krause C, S Rossi, M Thibeault-Martel, P-Y. Plourde. 2010. Relationships of climate and cell features in stems and roots of black spruce and balsam fir. *Annals of Forest Science* 67(4):402.
- Longui EL, KS Rajput, AC Galvão de Melo, LA Alves, CB Nascimento. 2017. Root to branch wood anatomical variation and its influence on hydraulic conductivity in five Brazilian Cerrado species. *Bosque* 38(1): 183-193. DOI: [10.4067/S0717-92002017000100018](https://doi.org/10.4067/S0717-92002017000100018)
- Longui EL, RABG Silva, D Romeiro, IL Lima, SMB Florsheim, ACG Melo. 2012. Root-branch anatomical investigation of *Eriotheca gracilipes* young trees: a biomechanical and ecological approach. *Scientia Forestalis* 40(93):23-33.
- Machado SR, Angyalossy-Alfonso V, BL Morretes. 1997. Comparative wood anatomy of root and stem in *Styrax camporum* (Styracaceae). *IAWA Journal* 18(1): 13-25. DOI: [10.1163/22941932-90001454](https://doi.org/10.1163/22941932-90001454)
- Machado SR, RA Rodella, V Angyalossy, CR Marcati. 2007. Structural variations in root and stem wood of *Styrax* (Styracaceae) from Brazilian forest and Cerrado. *IAWA Journal* 28(2): 173-188.
- Maeght JL, Rewald B, Pierret A. 2013. How to study deep roots—and why it matters. *Functional Plant Ecology* 4(299): 1-15. DOI: [10.3389/fpls.2013.00299](https://doi.org/10.3389/fpls.2013.00299)
- Marcati CR, J Sonsin-Oliveira, SR Machado. 2006. Growth rings in Cerrado woody species: occurrence and anatomical markers. *Biota Neotropica* v6(3). http://www.biotaneotropica.org.br/v6n3/pt/abstract?article+bn_00206032006
- Marcati CR, LR Longo, A Wiedenhoef, CF Barros. 2014. Comparative wood anatomy of root and stem of *Citharexylum myrianthum* (Verbenaceae). *Rodriguésia* 65(3): 567-576.
- Montefusco ARG. 2005. Anatomia Ecológica do Lenho de *Stryphnodendron adstringens* (Mart.) Coville (Leguminosae), Barbatimão, no Parque Estadual do Cerrado – Jaguariava-PR. Cutitiba, Brasil. Dissertação de Mestre em Ciências Florestais. Universidade Federal do Paraná. 105 p.
- Paula JE, FG Silva-Júnior, APP Silva. 2000. Caracterização anatômica de madeiras nativas de matas ciliares do centro-oeste brasileiro. *Scientia Forestalis* 58:73-89.
- Pratt RB, AL Jacobse, FW Ewer, SD Davis. 2007. Relationships among xylem transport, biomechanics and storage in stems and roots of nine Rhamnaceae species of the California chaparral. *New Phytologist* 174(4):787-798.
- Ratter JA, JF Ribeiro, S Bridgewater. 1997. The Brazilian Cerrado vegetation and threats to its biodiversity. *Annals of Botany* 80(3): 223-230.
- Richter HG, MJ Dallwitz. 2000 onwards. Commercial timbers: descriptions, illustrations, identification, and information retrieval. In English, French, German, and Spanish. Version: 25th June 2009. Accessed 5 Set. 2016. Available in <http://delta-intkey.com>
- Soffiatti P, V Angyalossy-Alfonso. 1999. Estudo anatômico comparativo do lenho e da casca de duas espécies de *Eugenia* L. (Myrtaceae). *Revista Brasileira de Botânica* 22(2): 175-184.
- Sonsin JO, P Gasson, SR Machado, C Caum, CR Marcati. 2014. Atlas da diversidade de madeiras do Cerrado paulista. Botucatu, Brasil. Fundação de Estudos e Pesquisas Agrícolas e Florestais. 423 p.
- Teixeira LL, PP Matos, Paulo César Botosso, RA Seitz, SM Salis. 2003. Anatomia de madeiras do Pantanal Mato-Grossense - Características microscópicas. Colombo, Brasil. Embrapa Florestas. 182 p.

Recibido: 20/04/18
Aceptado: 27/12/18

